

## Accepted Manuscript

Synthesis, crystal structure and DFT studies of a new dioxomolybdenum(VI) Schiff base complex as an olefin epoxidation catalyst

Zeinab Asgharpour, Faezeh Farzaneh, Alireza Abbasi, Mina Ghiasi

PII: S0277-5387(15)00532-X  
DOI: <http://dx.doi.org/10.1016/j.poly.2015.09.030>  
Reference: POLY 11544

To appear in: *Polyhedron*

Received Date: 8 July 2015  
Accepted Date: 5 September 2015

Please cite this article as: Z. Asgharpour, F. Farzaneh, A. Abbasi, M. Ghiasi, Synthesis, crystal structure and DFT studies of a new dioxomolybdenum(VI) Schiff base complex as an olefin epoxidation catalyst, *Polyhedron* (2015), doi: <http://dx.doi.org/10.1016/j.poly.2015.09.030>

This is a PDF file of an unedited manuscript that has been accepted for publication. As a service to our customers we are providing this early version of the manuscript. The manuscript will undergo copyediting, typesetting, and review of the resulting proof before it is published in its final form. Please note that during the production process errors may be discovered which could affect the content, and all legal disclaimers that apply to the journal pertain.



# Synthesis, crystal structure and DFT studies of a new dioxomolybdenum(VI) Schiff base complex as an olefin epoxidation catalyst

Zeinab Asgharpour<sup>a</sup>, Faezeh Farzaneh<sup>a\*</sup>, Alireza Abbasi<sup>b</sup>, Mina Ghiasi<sup>a</sup>

<sup>a</sup>Department of Chemistry, Faculty of Physics & Chemistry, Alzahra University, P.O.Box 1993891176, Vanak, Tehran, Iran

<sup>b</sup>School of Chemistry, College of Science, University of Tehran, P.O. Box 14155 6455, Tehran, Iran

## ABSTRACT

A cis-dioxomolybdenum(VI) complex was prepared from Mo(acac)<sub>2</sub> and a Schiff base ligand derived from 2-hydroxy-1-naphthaldehyde (Naph) and L-histidine (His) in ethanol and was designated as MoO<sub>2</sub>(Naph-His). Characterization of MoO<sub>2</sub>(Naph-His) was carried out by means of elemental analysis, <sup>1</sup>H NMR, <sup>13</sup>C NMR, FT-IR, UV-Vis and TGA techniques. The crystal structure of MoO<sub>2</sub>(Naph-His), determined by single-crystal X-ray crystallography, revealed that the coordination of Mo in the complex is a distorted octahedron, formed by a tetradentate Naph-His Schiff base ligand and two binding oxygen atoms. The optimized geometrical parameters obtained by DFT calculations are in good agreement with the single XRD data. It was found that MoO<sub>2</sub>(Naph-His) successfully catalyzes the epoxidation of cyclooctene, cyclohexene and norbornene with 80-100% conversions and 54-100% selectivities. Based on the obtained results, the heterogeneity and reusability of the catalyst seems promising.

**Keywords:** Mo complex, Schiff base ligand, epoxidation, alkenes

\*Corresponding author. Tel.: +98-21-88258977; fax: +98-21-+98-21-88041344;  
E-mail address: [faezeh\\_farzaneh@yahoo.com](mailto:faezeh_farzaneh@yahoo.com), Farzaneh@alzahra.ac.ir

## 1. Introduction

The enzymatic role of molybdenum compounds in biological reactions has created a tremendous impetus in the synthesis of a number of model complexes mimicking oxotransferase molybdoenzymes [1-4]. In this regard, many stable molybdenum complexes with oxygen-, nitrogen- and sulfur-containing ligands have been prepared. Molybdenum(VI) Schiff base complexes with a cis-MoO<sub>2</sub> core are excellent enzyme model systems for the active sites of molybdo-enzymes, such as xanthine oxidase, nitrogenase and sulfite oxidase. Possessing an Mo=O unit, they have widely been used as catalysts in industrial processes, such as epoxidation, sulfoxidation and hydroxylation of olefins, [5-9].

Coordination complexes of Mo with Schiff base ligands have wide applications in electrochemistry [10] and biological modelling [11], as antioxidant [12] and antibacterial agents [13], and as catalysts for hydrogen generation [14], alkene epoxidations [15,16] and sulfide oxidations [17]. In order to mimic biological systems, a number of dioxomolybdenum complexes have been synthesized and characterized [18-22]. The activity of these complexes varies with the ligand type and coordination sites. In spite of the synthesis of many Mo complex Schiff bases, there are few reports on the preparation of Schiff bases with amino acids [23-24]. Amino acids are efficient biologically active and cytotoxic agents and are considered as anticancer and antibacterial reagents [25,26]. Amino acid Schiff bases are sensitive to moisture and decompose when exposed to air. Therefore, they are usually generated immediately prior to use for complexation. It is particularly significant that isolated crystalline amino acid Schiff bases have rarely been reported [27].

The catalytic epoxidation of alkenes is a reaction of great industrial interest because epoxides are widely used as intermediate chemicals for making valuable products, such as chiral

pharmaceuticals, epoxy resins, epoxy paints, surfactants, pesticides, agrochemicals, perfume materials and sweeteners. Epoxides have also been numerously applied as precursors in the production of fine chemicals [28-34]. The type of ligand structure present in the complex and the catalytic reaction conditions have a significant effect on the catalytic activity of complexes involving the Mo(VI) metal center [35]. As a result, several research groups have focused on the design of new Mo(VI) complexes and their potential applications.

In this study, an attempt has been made to prepare a new Schiff base complex of Mo with His and Naph and using it as a catalyst for the epoxidation of some alkenes.

## 2. Experimental

### 2.1. Materials and characterization

All materials were of commercial reagent grade and used without further purification. *t*-Butyl hydroperoxide (TBHP) was purchased from Fluka, 2-hydroxy-1-naphthaldehyde (Naph), L-histidine (His), sodium acetate, hydrogen peroxide (30%), cyclooctene, diethyl ether and ethanol were purchased from Merck Chemical Company. FT-IR spectra were recorded on a Bruker Tensor 27 FT-IR spectrometer using KBr pellets over the range 4000-400  $\text{cm}^{-1}$ . The UV-Vis measurements were performed on a double beam UV-Vis Perkin Elmer Lambda 35 spectrophotometer. Single crystal measurement was performed on an Agilent Super Nova Dual single crystal diffractometer. Intensity data were collected using graphite monochromatised Mo  $K_{\alpha}$  radiation ( $k = 0.71073 \text{ \AA}$ ). Chemical analyses of samples were determined with a Perkin Elmer atomic absorption spectrometer (AAS). TGA thermal curve measurement was carried out with a Perkin Elmer Pyris 1. Oxidation products were analyzed by GC and GC-MS using an

Agilent 6890 Series with an FID detector, HP-5, 5% phenylmethyl siloxane capillary and an Agilent 5973 Network, mass selective detector, HP-5 MS 6989 Network GC system.

## 2.2. Preparation of $[MoO_2(Naph-His)]$

Initially, Naph (0.172 g, 1 mmol) was dissolved in ethanol (2 mL). This solution was then added to a solution of His (0.155 g, 1 mmol in 2 mL water). Upon addition of an aqueous sodium acetate solution (0.164 g, 2 mmol in 1 mL water), the color changed to yellow. To this solution was added  $MoO_2(acac)_2$  (0.278 g, 0.85 mmol in 2 mL ethanol, prepared according to the literature method [36]), followed by heating at reflux for 3 h. The yellow resultant solid was then filtered, washed with water, ethanol and diethyl ether, and then dried in air at room temperature. X-ray crystals of the complex  $[MoO_2(Naph-His)]$  were obtained by slow diffusion of diethyl ether into a saturated  $[MoO_2(Naph-His)]$  solution in  $CH_3CN/EtOH/CHCl_3$  (1:1:0.5).

Yield: 50%. Decomposition point: 297 °C. Anal. Calc. for  $C_{17}H_{13}MoN_3O_5$  ( $M = 435.24 \text{ g mol}^{-1}$ ): Mo, 22.04; C, 46.91; H, 3.01; N, 9.65. Found: Mo, 21.98; C, 46.90; H, 2.99; N, 9.63%. FT-IR (KBr pellet)  $cm^{-1}$ : 1625 (C=N), 1557, 1386 (COO), 1557 (C=C), 547 (Mo–O), 497 (Mo–N), 910, 920 (cis- $MoO_2$ ) [37,38]. UV-Vis(methanol)  $\lambda_{max}$  (nm): 270, 285, 346, 414 [39].  $^1H$  NMR (DMSO- $d_6$ )  $\delta$ , ppm: 3.19-3.24 (m) (b-CH), 7.11 (m) (imidazole-5-H), 7.56-7.69 (m) (Ar-H), 8.37 (d) (imidazole-2-H), 9.00 (s) (CH=N), 12.82 (brs) (imidazole N-H).  $^{13}C$  NMR (DMSO- $d_6$ )  $\delta$ , ppm: 116.0 (imidazole-C), 118.8 (Ar), 122.7 (Ar), 123.0 (Ar), 133.1 (A), 135.1 (imidazole-C), 136.8 (Ar), 162.5 (CH=N), 165.4 (Ar), 174.6 (C=O) [37].

## 2.3. General procedure for the oxidation of alkenes

All oxidation reactions of alkenes (norbornene, cyclohexene and cyclooctene) were carried out in a round bottom flask equipped with a magnetic stirrer and a water-cooled condenser. Typically, [MoO<sub>2</sub> (Naph-His)] as catalyst (0.025 g) in CCl<sub>4</sub> (5 mL) and alkene (10 mmol) with TBHP (14 mmol) were mixed and the mixture was heated at reflux for 8 h. After separation of the catalyst, the filtrate was subjected to GC and GC-Mass for analyses.

#### 2.4. X-ray crystallography

Crystallographic data were collected on a MAR345 dtb diffractometer equipped with image plate detector using Mo-K $\alpha$  radiation (0.71073 Å). The structure was solved by direct methods using SHELXS-97 and refined using the full-matrix least-squares method on  $F^2$ , SHELXL-97 [40]. All non-hydrogen atoms were refined anisotropically. Hydrogen atoms were added at ideal positions and refined using a riding model. Crystallographic data, details of collected data and structure refinement are listed in Table 1. Selected bond lengths and angles are shown in Table 2.

#### 2.5. Computational details

All calculations were carried out with the Gaussian program series 2003 [41]. The optimization of the geometry was performed employing a hybrid Hartree-Fock-density functional scheme, the adiabatic connection method-Becke three-parameter with Lee-Yang-Parr (B3LYP) [42] density functional theory (DFT) [43] with the two standard 3-21G and 6-31G\* basis sets. Full optimizations were performed without any symmetry constraints. The harmonic vibrational frequencies were computed to confirm that an optimized geometry correctly corresponds to a local minimum that has only real frequencies. The partial charges were obtained using the NBO method. The solvent effect was investigated with the PCM method [44] at the B3LYP/6-31G\*

level. Solvation calculations were carried out for ethanol with the geometries optimization for this solvent.

### 3. Results and discussion

#### 3.1. Synthesis and characterization of [MoO<sub>2</sub>(Naph-His)] (**1**)

The complex [MoO<sub>2</sub>(Naph-His)] (**1**) was prepared in high yield and purity by the combination of an ethanol solution of MoO<sub>2</sub>(acac)<sub>2</sub> with His and Naph in a stoichiometric ratio of 1:1 under reflux conditions (Scheme 1). The obtained complex was readily recrystallized by diffusion of ether into a solution of the complex. It is soluble in ethanol, methanol, acetonitrile, dimethyl formamide (DMF) and dimethyl sulfoxide (DMSO), but insoluble in aliphatic solvents. The complex was characterized by FT-IR, UV-Vis, Mass, <sup>1</sup>H and <sup>13</sup>C NMR spectroscopy, TGA, elemental analysis and X-ray crystallography. Elemental analysis results of complex **1** were found to be entirely consistent with its composition as determined by X-ray crystallography.

An ORTEP view (50% thermal ellipsoids) of [MoO<sub>2</sub>(Naph-His)] is shown in Fig. 1. This complex crystallizes in the orthorhombic system, space group *p*2<sub>1</sub>2<sub>1</sub>2 with *Z* = 4 (Table 1). The metal ion is surrounded by 4 oxygen and 2 nitrogen atoms in a severely distorted octahedral geometry, with bond angles varying from 73.1(2) to 105.7(2)°. The molybdenum center is bonded to two terminal oxido groups, Mo=O4 and Mo=O5, equidistance at 1.70(1) Å and with an O=Mo=O angle of 105.7(2)°, which is in the usual range for cis-MoO<sub>2</sub> complexes [45].

The tetradentate Schiff base ligand coordinates to the molybdenum MoO<sub>2</sub><sup>2+</sup> unit via two imine N atoms and deprotonated carboxylic acid and phenoxy O atoms [N1, N2, O1, O3]. The oxygen donors (O1 and O3) are *trans* to each other and form one five and one six membered ring with one nitrogen donor (N1). Moreover, the N1 and N2 atoms are *trans* to the oxo groups (O4 and O5), leading to relatively long Mo-N bond distances (Mo-N1 = 2.21(1) Å, Mo-N2 = 2.36(1) Å),

due to oxo *trans* influence, as previously observed for other dioxo molybdenum(VI) complexes [46]. The molybdenum atom deviates towards the axial O4 oxygen atom by 0.284 Å from the O5, O1, O3, N1 plane. This phenomenon is common in related cis-MoO<sub>2</sub> octahedral complexes [47]. In the solid structure of the [MoO<sub>2</sub>(Naph-His)] complex, four hydrogen bonding, C-H... $\pi$  and  $\pi$ ... $\pi$  interactions are important for building up the three-dimensional network (Fig. 2). In the complex, the hydrogen atoms H2 and H14B of C2 and C14, respectively, belonging to the Schiff base ligand show two different relatively weak hydrogen bonding interactions with two different O4 oxido atoms. Another hydrogen atom, attached to the imine N3 atom, is hydrogen bonded to the O1 and O2 atoms of two Schiff base ligands from two neighboring molecules. As a result, these four hydrogen bonds are responsible for connecting each molecule to four neighboring molecules. Details of the hydrogen bonds are summarized in Table 3. Moreover, C-H... $\pi$  and  $\pi$ ... $\pi$  interactions exist between C6-H6...Cg5 (3.58 Å) and Cg6...Cg6 (3.60 Å) (Cg5 being the ring C4/C5/C6/C7/C8/C9 and Cg6, C8/C9/C10/C11/C12/C13) in neighboring molecules, stabilizing the 3D framework (Fig. 2).

The FT-IR spectra of the (Naph-His) Schiff base ligand and [MoO<sub>2</sub>(Naph-His)] complex are shown in Figs. 3a and b, respectively. As seen in Fig. 3a, whereas the C=N stretching band of the free ligand appears at 1635 cm<sup>-1</sup>, it shifts to lower frequency (1625 cm<sup>-1</sup>) after complexation (Fig. 3b), indicating that the imine lone pair is involved in bonding to the metal ion. The bands appearing at 1557 and 1386 cm<sup>-1</sup> should be attributed to the asymmetric and symmetric stretching vibrations of the COO<sup>-</sup> group. Two characteristic peaks displayed at 920 and 910 cm<sup>-1</sup> are assigned to the Mo=O band in [MoO<sub>2</sub>(Naph-His)] [48]. Two other bands appearing at 547 and 497 cm<sup>-1</sup> are due to the Mo–O and Mo–N vibrations, indicating that complexation of Mo occurs with the phenol oxygen and azomethine nitrogen atoms, respectively [49].



The thermal decomposition of the  $[\text{MoO}_2(\text{Naph-His})]$  complex was studied to evaluate its thermal stability. As seen in Fig. S1 (see supplementary data), the TGA/DTA curves of the complex show thermal stability up to 300 °C. A one step weight loss at 380 °C, along with exothermic peaks in the DTA curve, is due to the decomposition of the organic ligand (obs.: 71.80%, calc.: 71.52%) with the formation of molybdenum oxide. The other point shows the starting decomposition at 400 °C, consistent with decomposition point of the  $[\text{MoO}_2(\text{Naph-His})]$  complex.

The UV-Vis spectra of the ligand and the Mo complex in ethanol are shown in Fig. 4. The electronic spectrum of the Schiff base ligand exhibits three main peaks at 222 ( $\epsilon = 19 \times 10^3 \text{ M}^{-1} \text{ cm}^{-1}$ ), 236 ( $\epsilon = 16 \times 10^3 \text{ M}^{-1} \text{ cm}^{-1}$ ) and 311 nm ( $\epsilon = 4 \times 10^3 \text{ M}^{-1} \text{ cm}^{-1}$ ) (Fig. 4). The first and second peaks are attributed to the naphthaldehyde  $\pi \rightarrow \pi^*$  and imine  $\pi \rightarrow \pi^*$  transitions, respectively. These bands were slightly affected by chelation and shifted to longer wavelength. The third band is assigned to the azomethine  $n \rightarrow \pi^*$  transition. This band was shifted to longer wavelength at 326 nm, together with increased intensity. This shift may be attributed to the nitrogen atom lone pair donation of the Schiff base to the metal ion [50]. The absorption maximum, appearing at 386 nm, can be assigned to  $\text{N} \rightarrow \text{M}$  and  $\text{O} \rightarrow \text{M}$  ligand to metal charge transfer (LMCT) transitions [51].

The  $^1\text{H}$  and  $^{13}\text{C}$  NMR spectra of the Schiff base ligand and  $[\text{MoO}_2(\text{Naph-His})]$  are shown in Figs. S2-S3 and Figs. S4-S5, respectively (see supplementary data). The characteristic sharp azomethane N-H signal of the ligand, which appears at 8.48 ppm (Fig. S2), shifts to 12.8 ppm in the  $^1\text{H}$  NMR spectrum of  $[\text{MoO}_2(\text{Naph-His})]$  (Fig. S4). On the other hand, the ligand acidic proton, displayed at 13.6 ppm (Fig. S2), disappears in the  $^1\text{H}$  NMR spectrum of  $[\text{MoO}_2(\text{Naph-His})]$  (Fig. S4) due to complexation of the  $\text{CO-O}^-$  group to the metal center. The  $^{13}\text{C}$  NMR

spectrum of  $[\text{MoO}_2(\text{Naph-His})]$  exhibits 2 aliphatic, 14 aromatic and 1 CO carbon signals, consistent with the molecular structure of  $[\text{MoO}_2(\text{Naph-His})]$  (Fig. S5).

### 3.2. Theoretical section:

#### 3.2.1 Geometry optimization of the (Naph-His) Schiff base ligand

The structure of the Naph-His Schiff base ligand was fully optimized by the B3LYP method using two basis set, including 3-21G and 6-31\*, with no initial symmetry restrictions and assuming the  $C_1$  point group. The optimized geometry of the ligand and some structural details are given in Fig. S6 and Table S1, respectively (see supplementary data). Calculation of the vibrational frequencies has confirmed a stationary point with no negative eigenvalue observed in the force constant matrix.

#### 3.2.2. Geometry optimization of the $[\text{MoO}_2(\text{acac})_2]$ and $[\text{MoO}_2(\text{Naph-His})]$ complexes

According to equation 1, the model compound  $[\text{MoO}_2(\text{Naph-His})]$  used in this study was generated when one optimized (Naph-His) molecule comes close to the optimized  $[\text{MoO}_2(\text{acac})_2]$  complex:



The optimized structure of the  $[\text{MoO}_2(\text{acac})_2]$  complex together with some structural details and the optimized structure of  $[\text{MoO}_2(\text{Naph-His})]$  are shown in Figs. S7, S8 and Table S2 (see supplementary data). In order to compare the reliability of our predicted results, a comparison between the theoretical and experimental data is presented in Table 2. As indicated in this Table, the standard deviation of bond distances, bond angles and dihedral angles for the B3LYP/3-21G and B3LYP/6-31G\* levels are very similar. In fact, there is a good agreement between the solid structure and gas phase calculated values, the small differences are due to the X-ray crystal

diffraction being applied in the solid state. Recall that calculations were performed in the gas state.

To reduce the computational cost, the B3LYP method with the 3-21G basis set can be applied to optimize the molybdenum complexes. Calculation of vibrational frequencies has confirmed a stationary point with no negative eigenvalue observed in the force constant matrix.

In the next step, the fully optimized geometry of the  $[\text{MoO}_2(\text{Naph-His})]$  complex in the gas phase was re-optimized by considering the solvent effect ( $E = 431569.12$  Kcal/mol) using the PCM method. The calculated results indicated that the complex is stabilized by 38.5 kcal/mol in ethanol, perhaps due to rather high complex dipole moment (10.41 D).

### 3.2.3. Details of atomic net charge

The calculated net charges on the  $[\text{MoO}_2(\text{Naph-His})]$  complex are given in Table S3 (see supplementary data). These partial charges are derived from natural bond orbital (NBO) calculations. The net negative charges on O1(-0.550), O2(-0.481), O3(-0.619), O4(-0.363), N1(-0.604), N2(-0.625) and N3(-0.550) in the Naph-His molecule are reported in Table S3. Of particular significance is the partial charge of 1.19 observed on the molybdenum atom when Naph-His is coordinated. In fact, the calculated electron density computed on the donor oxygen and nitrogen atoms is less than expected, while the electron density computed on the central ion is more than expected. Thus, the net charge results confirm an electron transmission from the donor atoms of the Naph-His ligand to the central Mo ion.

### 3.2.5. Molecular orbital analysis point of view

To find the nature of binding between the Naph-His ligand and  $\text{Mo}^{2+}$ , molecular orbital (MO) analysis has been employed. This analysis is useful in presenting the factors influencing the

stability of this complex. Taking into account the above discussion, we focused mostly on the  $[\text{MoO}_2(\text{Naph-His})]$  complex. The highest occupied molecular orbital (HOMO) and lowest unoccupied molecular orbital (LUMO) of the  $[\text{MoO}_2(\text{Naph-His})]$  complex are shown in Fig. 5. While the LUMO is mainly based on molybdenum 3d orbitals, the HOMO includes contributions from both  $\text{Mo}^{2+}$  and interacting ligand heteroatoms. The presented HOMO orbital reveals an antibonding interaction between the metal ion and ligand orbitals. These antibonding molecular orbitals arise from the interaction between the  $d\sigma$  metal orbital and the lone pairs of ligand oxygen atoms.

### 3.3. Catalytic studies

In order to evaluate the catalytic activity of  $[\text{MoO}_2(\text{Naph-His})]$  in epoxidation reactions, cyclooctene was selected as a model alkene. For this reaction, the effects of the amount of catalyst, time and solvent were studied (Figs. 7-9). As indicated in Fig. 7, increasing the amount of catalyst from 10 to 25 mg increases the conversion from 37 to 100% with 100% selectivity. Therefore, all epoxidation reactions were carried out using 25 mg of catalyst. Similarly, increasing the reaction time from 1 to 8 h using 25 mg of catalyst was found to increase the cyclooctene conversion from 23 to 100% with 100% selectivity (Fig. 8). To test the effect of solvent, the epoxidation reaction was carried out in different solvents (Fig. 9). The trend of activity was found to be  $\text{CCl}_4 > \text{CHCl}_3 > \text{CH}_2\text{Cl}_2 > \text{n-hexane} > \text{ethanol} > \text{CH}_3\text{CN}$ . It is evident that while coordinating solvents inhibited the reaction completely (ethanol or  $\text{CH}_3\text{CN}$ ), epoxidation proceeded in non-coordinating solvents ( $\text{CH}_2\text{Cl}_2$ ,  $\text{CHCl}_3$  or  $\text{CCl}_4$ ). Based on the conversion percentage,  $\text{CCl}_4$  was found to be the best solvent. Since  $\text{CCl}_4$  has the highest boiling point within these three solvents, a higher rate based on the Arrhenius equation is expected. Beside boiling point, decreasing polarity from  $\text{CH}_2\text{Cl}_2$  to  $\text{CHCl}_3$  and  $\text{CCl}_4$  may not be

overlooked. As such, the epoxidation transition state seems to be less polar than the starting material since such reactions should be decelerated in a more polar solvent ( $\text{CH}_2\text{Cl}_2$ ) in comparison to a less polar solvent ( $\text{CCl}_4$ ) [52].

Epoxidation of norbornene and cyclohexene with TBHP was then carried out with  $[\text{MoO}_2(\text{Naph-His})]$  as the catalyst in  $\text{CCl}_4$  under the optimum reaction conditions (Fig. 10). We have included the cyclooctene epoxidation results in Fig. 10 in order to make a comparison more convenient. As seen in this Figure, the alkene epoxidation reactions proceeded with 80-100 % conversions and 54-100% selectivities.

To give an insight into the reaction mechanism, epoxidation of cyclooctene was carried out in the presence of diphenylamine as a radical scavenger. Observation of suppression of the epoxidation yield clearly revealed that this reaction has proceeded via a radical mechanism [53,54]. Based on the operation of a radical mechanism, one may rationalize the results obtained in Fig. 10. Whereas cyclooctene exclusively gives the corresponding epoxide, cyclohexene undergoes allylic oxidation and epoxidation, concomitantly (Fig. 10.). It has been reported that the high epoxidation selectivity typically observed for cyclooctene is related to a poor  $\sigma_{\text{C-}\alpha\text{H}}-\pi_{\text{C}=\text{C}}$  orbital overlap in the predominant conformation, disfavoring  $\alpha\text{H}$ -abstraction by radical species (Scheme 2a) [55]. Therefore, allylic-site oxidation of cyclooctene is not in competition with epoxidation. On the other hand, cyclohexene exist in the half-chair conformation in which allylic carbons lie in the plane of the double bond (Scheme 2b) [56]. Therefore, cyclohexene undergoes two competing oxidations, epoxidation and allylic-site. Norbornene is particularly significant, selectively affording the corresponding epoxide (Fig. 10). If norbornene undergoes allylic-site oxidation through  $\alpha\text{H}$ -abstraction by radical species, it affords a bridgehead radical which has

been shown to be unstable due to Bredt's rule (Scheme 2c) [57]. Therefore, norbornene conclusively undergoes an epoxidation reaction, affording the corresponding epoxide.

The recyclability of the  $[\text{MoO}_2(\text{Naph-His})]$  complex as a catalyst was investigated under the optimum reaction conditions. After each reaction cycle, the catalyst was recovered by centrifugation, washed several times with ethanol and dried under vacuum. Catalyst activity was found to be unchanged (100% conversion and 100% selectivity) after three runs, beyond which a slight decrease in conversion (98%) was observed, but with 100% selectivity after five runs. Since no catalytic activity was observed when the filtrate of each run was subjected to the epoxidation conditions in the absence of catalyst, it can be concluded that the catalyst is truly functioning heterogeneously in nature.

#### 4. Conclusion

In this study, a dioxomolybdenum(VI) complex was prepared with the tetradentate 2-hydroxy naphthaldehyde-L-histidin (Naph-His) Schiff base ligand. The molecular structure of the complex was determined by single-crystal X-ray crystallography. The Mo atom in the  $[\text{MoO}_2(\text{Naph-His})]$  complex was found to have adopted a severely distorted octahedral 6-coordinated geometry and with two terminal oxido groups as  $\text{Mo}=\text{O}$  bonds. The optimized geometrical parameters obtained by DFT calculations are in good agreement with the single XRD data. We have also demonstrated the effectiveness of the  $[\text{MoO}_2(\text{Naph-His})]$  complex as a catalyst for the epoxidation of some alkenes with TBHP. Easy preparation, mild reaction conditions and rather high yield cyclooctene and norbornene epoxidation reactions with 100% selectivity demonstrate that the  $[\text{MoO}_2(\text{Naph-His})]$  complex is a useful catalyst.

## Appendix A. Supplementary data

CCDC 1001623 contains the supplementary crystallographic data for  $C_{17}H_{13}MoN_3O_5$ . These data can be obtained free of charge via <http://www.ccdc.cam.ac.uk/conts/retrieving.html> or from the Cambridge Crystallographic Data Centre, 12 Union Road, Cambridge CB2 1EZ, UK; fax: (+44) 1223-336-033; or e-mail: [deposit@ccdc.cam.ac.uk](mailto:deposit@ccdc.cam.ac.uk).

## Acknowledgements

Financial support from the Alzahra University is gratefully acknowledged.

## References

- [1] A. Majumdar, S. Sarkar, *Coord. Chem. Rev.* 255 (2011) 1039.
- [2] R.H. Holm, E.I. Solomon, A. Majumdar, A. Tenderholt, *Coord. Chem. Rev.* 255 (2011) 993.
- [3] S. Metz, W. Thiel, *Coord. Chem. Rev.* 255(2011) 1085.
- [4] R.H. Holm, *Chem. Rev.* 87 (1987) 1401.
- [5] C.J. Doonan, H.L. Wilson, K.V. Rajagopalan, R.M. Garrett, B. Bennett, R.C. Prince, G. N. George, *Am. Chem. Soc.* 129 (2007) 9421.
- [6] A. Maghalom, J.G. Fedor, A. Walburger, J.H. Weiner, *Coord. Chem. Rev.* 255 (2011) 1159.
- [7] M. Bagherzadeh, M. Amini, H. Parastar, M. Jalali-Heravi, A. Ellern, L. K. Woo, *Inorg. Chem. Commun.* 20 (2012) 86.
- [8] Y. S. X. Zenga, X. Fang, X. Fub, Y. Xiao, L. Chend, M. Li, S. Chenga, *J. Mol. Catal. A-Chem.* 270 (2007) 61.
- [9] M. Bagherzadeh, R. Latifi, L. Tahsini, V. Amani, A. Ellern, L. K. Woo, *Polyhedron* 28 (2009) 2517.
- [10] N. K. Ngan, K.M. Lo, C.S.R. Wong, *Polyhedron* 2012 (2012) 235.

- [11] J. Q. Xie, C.H. Li, J.X. Dong, W. Qu, L.Pan, M.L. Peng, M.A. Xie, X. Tao, C. M. Yu, Y. Zhu, P.H. Zhang, C.G. Tang, Q.G. Li, *Thermochim. Acta* 598 (2014) 7.
- [12] M. Ikram, S. Rehman, A. Khan, R.J. Baker, T.S. Hofer, F. Subhan, M. Qayum, Faridoon, C. Schulzke, *Inorg. Chim. Acta* 428 (2015) 117.
- [13] O. A. M. Ali, S. M. El-Medani, D. A. Ahmed, D. A. Nassar, *J. Mol. Struct.* 1074 (2014) 713.
- [14] J.-P. Cao, L.-L. Zhou, L.-Z. Fu, J.-X. Zhao, H.-X. Lu, S.-Z. Zhan, *Catal. Commun.* 57(2014) 1.
- [15] J. Zhang, P. Jiang, Y. Shen, W. Zhang, X. Li, *Microporous Mesoporous Mater.* 206 (2015) 161.
- [16] S. Rayati, N. Rafiee, A. Wojtczak, *Inorg. Chim. Acta* 386 (2012) 27.
- [17] E. Zamanifar, F. Farzaneh, J. Simpson, M. Maghami, *Inorg. Chim. Acta* 414 (2014) 63.
- [18] G.J. Chen, J.W. McDonald, W. Newton, *Inorg. Chem.* 15 (1976) 2612.
- [19] L. Casella, M. Gullotti, A. Pintar, S. Colonna, A. Manfredi, *Inorg. Chim. Acta* 144 (1988) 89.
- [20] J. Costa Pessoa, I. Cavaco, I. Correia, M.T. Duarte, R.D. Gillard, R.T. Henriques, F.J. Higes, C. Madeira, I. Tomaz, *Inorg. Chim. Acta* 293 (1999) 1.
- [21] R. Ando, H. Inden, M. Sugino, H. Ono, D. Sakaeda, T. Yagyu, M. Maeda, *Inorg. Chim. Acta* 357 (2004) 1337.
- [22] Q. Liu, Y. Yang, W. Hao, Z. Xu, L. Zhu, *IERI Procedia* 5 (2013) 178.
- [23] M. Gómez, S. Jansat, G. Muller, G. Noguera, H. Teruel, V. Moliner, E. Cerrada, M. Hursthouse, *Eur. J. Inorg. Chem.* 4 (2001) 1071.
- [24] R. Takjoo, M. Ahmadi, A. Akbari, H. Amiri Rudbari, F. Nicoloi, *J. Coord. Chem.* 65 (2012) 3403.
- [25] T.M. Aminabhavi, N.S. Biradar, S.B. Patil, V.L. Roddabasanagoudar, W.E. Rudzinski, *Inorg. Chim. Acta* 107 (1985) 231.
- [26] M. Gharagozlou, D.M. Boghaei, *Spectrochim. Acta A* 71 (2008) 1617.
- [27] P. Gürkan, N. Sari, *Synth. React. Inorg. Met.-Org. Chem.* 29 (1999) 753.
- [28] A. K. Yudin, J. B. Sweeney, *Aziridines and epoxides in organic synthesis*, Wiley-VCH Verlag GmbH & Co. KGaA, Weinheim, FRG, 2006.



- [29] G. Sienel, R. Rieth, K.T. Rowbottom, Epoxides. Ullmann's Encyclopedia of Industrial Chemistry, Wiley-VCH Verlag GmbH & Co. KGaA, Weinheim, FRG, 2000.
- [30] X.-H. Lu, Q.-H. Xia, H.-J. Zhan, H.-X. Yuan, C.-P. Ye, K.-X. Su, G. Xu, J. Mol. Catal. A 250 (2006) 62.
- [31] G. Xu, Q.-H. Xia, X.-H. Lu, H.-J. Zhan, J. Mol. Catal. A: Chem. 266 (2007) 180.
- [32] B. Qi, X.-H. Lu, S.-Y. Fang, J. Lei, Y.-L. Dong, D. Zhou, Q.-H. Xia, J. Mol. Catal. A: Chem. A 334 (2011) 44.
- [33] F. Farzaneh, Y. Sadeghi, J. Mol. Catal. A 398 (2015) 275.
- [34] J. Zhang, P. Jiang, Y. Shen, W. Zhang, X. Li, Micropor. Mesopor Mater. 206 (2015) 161.
- [35] K. Gupta, A.K. Sutar, and C.-C. Lin, Coord. Chem. Rev. 253 (2009) 1926.
- [36] G.J. Chen, J.W. McDonald, W. Newton, Inorg. Chem. 15 (1976) 2612.
- [37] L. Casella, M. Gullotti, A. Pintar, S. Colonna, A. Manfredi, Inorg. Chim. Acta. 144 (1988) 89.
- [38] J. Costa Pessoa, I. Cavaco, I. Correia, M.T. Duarte, R.D. Gillard, R.T. Henriques, F.J. Higes, C. Madeira, I. Tomaz, Inorg. Chim. Acta 293 (1999) 1.
- [39] R. Ando, H. Inden, M. Sugino, H. Ono, D. Sakaeda, T. Yagyu, M. Maeda, Inorg. Chim. Acta 357 (2004) 1337.
- [40] G. Sheldrick, SHELX-97, Program for the solution and refinement of crystal structures. University of Göttingen, Germany, 1997.
- [41] M.J. Frisch, G.W. Trucks, H. B. Schlegel, G.E. Scuseria, M.A. Robb, J.R. Cheeseman, V.G. Zakrzewski, J.A. Montgomery, R.E. Stratmann, J.C. Burant, S. Dapprich, J.M. Millam, A.D. Daniels, K.N. Kudin, M.C. Strain, O. Farkas, J. Tomasi, V. Barone, M. Cossi, R. Cammi, B. Mennucci, C. Pomelli, C. Adamo, S. Clifford, J. Ochterski, G.A. Petersson, P.Y. Ayala, Q. Cui, K. Morokuma, D.K. Malick, A.D. Rabuck, K. Raghavachari, J.B. Foresman, J. Cioslowski, J. V. Ortiz, B.B. Stefanov, G. Liu, A. Liashenko, P. Piskorz, I. Komaromi, R. Gomperts, R.L. Martin, D.J. Fox, T. Keith, M.A. Al-Laham, C.Y. Peng, A. Nanayakkara, C. Gonzalez, M. Challacombe, P.M. W. Gill, B.G. Johnson, W. Chen, M.W. Wong, J.L. Andres, M. Head-Gordon, E.S. Replogle, J.A. Pople, Gaussian 98 (Revision A.1), Gaussian, Inc., Pittsburgh PA, 1998.
- [42] A.D. Becke, J. Chem. Phys. 98 (1993) 5648.

- [43] R.G. Parr, R.G.P.W. Yang, Density-functional theory of atoms and molecules. 1989, Oxford University press.
- [44] V. Barone, M. Cossi, J. Tomasi, J. Comput. Chem. 19 (1998) 404.
- [45] S. Duman, I. Kızılcıklı, A. Koca, M. Akkurt, B. Ulküseven, Polyhedron 29 (2010) 2924.
- [46] M. Gómez, S. Jansat, G. Muller, G. Noguera, H. Teruel, V. Moliner, E. Cerrada, M. Hursthouse, Eur. J. Inorg. Chem. 4 (2001) 1071.
- [47] R. Takjoo, M. Ahmadi, A. Akbari, H. Amiri Rudbari, F. Nicoloi, J. Coord. Chem. 65 (2012) 3403.
- [48] O. Rajan, A. Chakravorty, Inorg. Chem. 20 (1981) 660.
- [49] G. Wang, J.C. Chang, Syn. React. Inorg. Met. 24 (1994) 1091.
- [50] B. Ghose, K. Lasisi, Syn. React. Inorg. Met. 16 (1986) 1121.
- [51] N. S. Rao, M.N. Jaiswal, D.D. Mishra, R.C. Maurya, N. Nageswara Rao, Polyhedron 2 (1993) 2045.
- [52] T. H. Lowry, K. S. Richardson, Mechanism and Theory in Organic Chemistry, 3<sup>rd</sup> Ed., Harper & Row, New York 1987, p. 361.
- [53] L. M. Slaughter, J. P. Collman, T. A. Eberspacher, J. I. Brauman, Inorg. Chem. 43 (2004) 5198.
- [54] F. Farzaneh, J. Taghavi, R. Malakooti, M. Ghandi, J. Mol. Catal. A- Chem, 244 (2006) 252.
- [55] U. Neuenschwander, I. Hermans, J. Org. Chem. 76 (2011) 10236.
- [56] E. L. Eliel, S. H. Wilen, Stereochemistry of Organic Compounds, 1994, John Wiley & Sons, Inc. New York. 726.
- [57] J. March, Advanced Organic Chemistry, 3<sup>rd</sup> ed. 1985, John Wiley & Sons, Inc. New York. p. 616.

**Figure captions:**

**Fig. 1.** Structure of  $[\text{MoO}_2(\text{Naph-His})]$ ; atomic numbering with ellipsoids drawn at the 50% probability level are shown.

**Fig. 2.** Packing structure of  $[\text{MoO}_2(\text{Naph-His})]$ . Hydrogen bonds (dashed tubes),  $\text{C(H)}\dots\pi(\text{C})$  interactions (pink tubes) and  $\pi$ - $\pi$  stacking interactions (green tubes).

**Fig. 3.** FT-IR spectra of (a) the Schiff-base ligand (Naph-His), (b) the  $[\text{MoO}_2(\text{Naph-His})]$  complex.

**Fig. 4.** Electronic spectrum of  $[\text{MoO}_2(\text{Naph-His})]$  in ethanol.

**Fig.5** Generation of the  $[\text{MoO}_2(\text{Naph-His})]$  complex.

**Fig.6.** The HOMO and LUMO views of the  $[\text{Mo}(\text{Naph-His})(\text{O}_2)]$  complex.

**Fig. 7.** The effect of the amount of catalyst on cyclooctene epoxidation.

**Fig. 8.** The effect of the reaction time on cyclooctene epoxidation.

**Fig. 9.** The effects of solvent on the epoxidation of cyclooctene.

**Fig. 10.** Epoxidation of different substrates, (reaction conditions: 10 mmol substrate, 12 mmol TBHP, solvent  $\text{CCl}_4$  (5 ml), catalyst 20 mg, time 8 h).

**Scheme 1.** Preparation of the  $[\text{MoO}_2(\text{Naph-His})]$  complex.

**Scheme 2.** Reactivity of alkenes with *tert*-BuOO $\cdot$  and *tert*-BuO $\cdot$

**Table 1**Selected crystallographic data for the [MoO<sub>2</sub>(Naph-His)] complex

Empirical formula	C <sub>17</sub> H <sub>13</sub> MoN <sub>3</sub> O <sub>5</sub>
Formula weight	434.24
Temperature (K)	293(2)
Wavelength (Å)	0.71073
Crystal system	orthorhombic
space group	<i>P</i> 2 <sub>1</sub> 2 <sub>1</sub> 2
<i>a</i> (Å)	7.6421(15)
<i>b</i> (Å)	15.405(3)
<i>c</i> (Å)	13.828(3)
<i>V</i> (Å <sup>3</sup> )	1627.9(6)
<i>Z</i>	4
Absorption coeff. (mm <sup>-1</sup> )	0.842
<i>D<sub>x</sub></i> (Mg m <sup>-3</sup> )	1.776
<i>R</i> <sub>int</sub>	0.0422
$\theta$ Range for collection (°)	1.98-26.00
Index ranges	-9 ≤ <i>h</i> ≤ 9 -19 ≤ <i>k</i> ≤ 18 -16 ≤ <i>l</i> ≤ 17
Reflections collected	9752
Independent reflections	3205
Independent reflections [ <i>I</i> > 2σ ( <i>I</i> )]	3046
Data / restraints / parameters	3205 / 0 / 205
Final <i>R</i> indices [ <i>I</i> > 2σ ( <i>I</i> )]	<i>R</i> 1 = 0.0366 <i>wR</i> 2 = 0.0754
<i>R</i> indices (all data)	<i>R</i> 1 = 0.0416 <i>wR</i> 2 = 0.0778

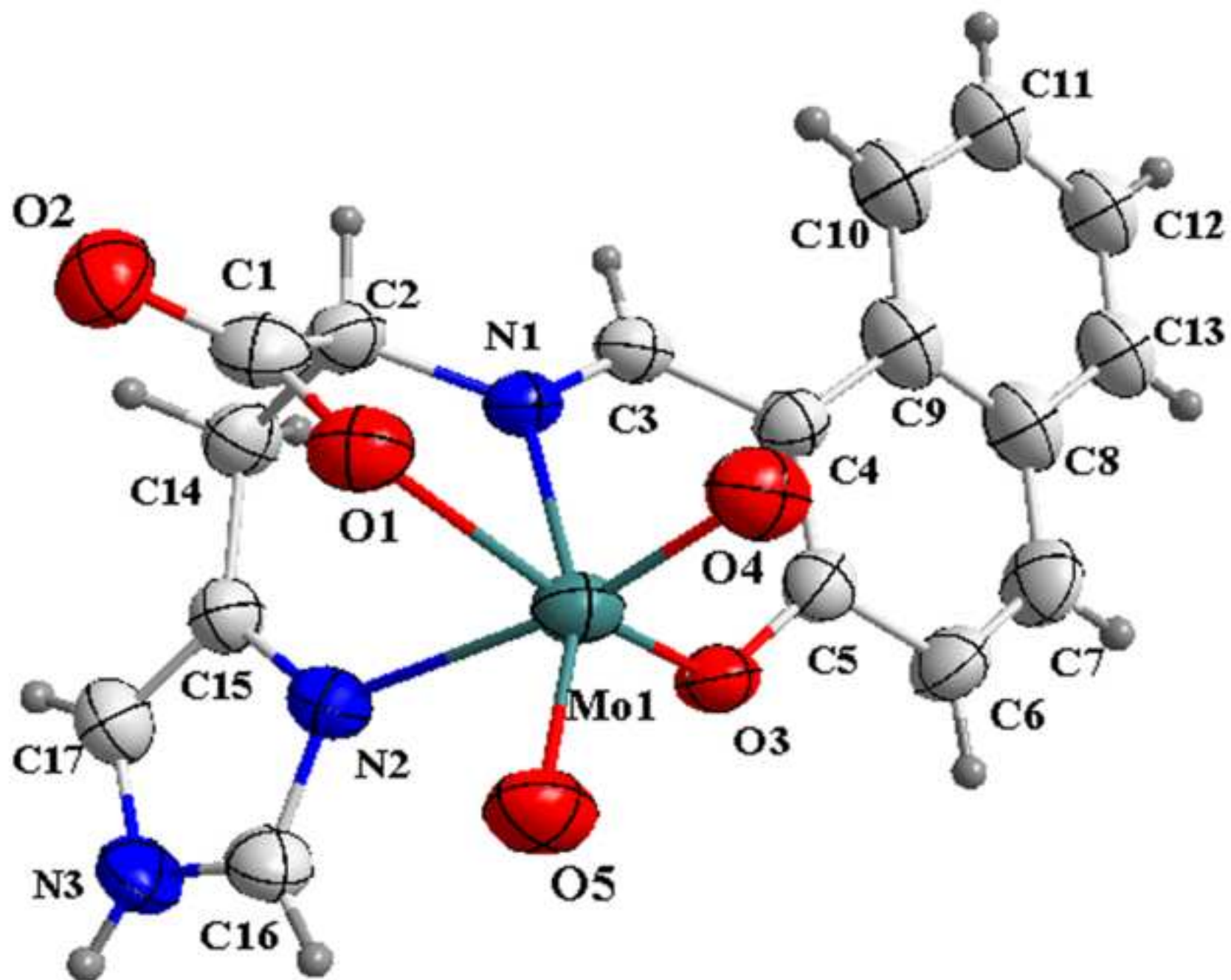
**Table 2**

Selected experimental (Exp.) and calculated (B3LYP/3-21G and B3LYP/6-31g\*) bond lengths (Å) and angles (°) for [MoO<sub>2</sub>(Naph-His)].

Connected Atom	Exp.	B3LYP/3-21G	B3LYP/6-31g*
Bond distance (Å)			
Mo—O <sub>5</sub>	1.696	1.739	1.70
Mo—O <sub>4</sub>	1.696	1.728	1.71
Mo—O <sub>3</sub>	1.941	1.999	2.00
Mo—O <sub>1</sub>	2.048	2.005	2.00
Mo—N <sub>1</sub>	2.205	2.261	2.21
Mo—N <sub>2</sub>	2.357	2.432	2.32
Standard deviation		0.12	0.085
Bond Angle (°)			
O <sub>5</sub> —Mo—O <sub>4</sub>	105.70	106.08	106.00
O <sub>5</sub> —Mo—O <sub>3</sub>	103.63	98.83	100.20
O <sub>4</sub> —Mo—O <sub>3</sub>	96.48	96.14	96.50
O <sub>5</sub> —Mo—O <sub>1</sub>	98.85	102.99	100
O <sub>4</sub> —Mo—O <sub>1</sub>	94.02	96.40	95.12
O <sub>5</sub> —Mo—N <sub>1</sub>	158.02	153.29	155.20
O <sub>4</sub> —Mo—N <sub>1</sub>	95.41	100.61	98.30
Standard deviation		9.77	5.56
Dihedral Angle (°)			
O4-Mo-O1-C1	116.2	117.7	117.0
O5-Mo-O1-C1	-137.3	-134.64	-135.5
N1-Mo-O1-C1	21.7	17.93	20.12
N2-Mo-O1-C1	-56.2	-57.53	-55.3

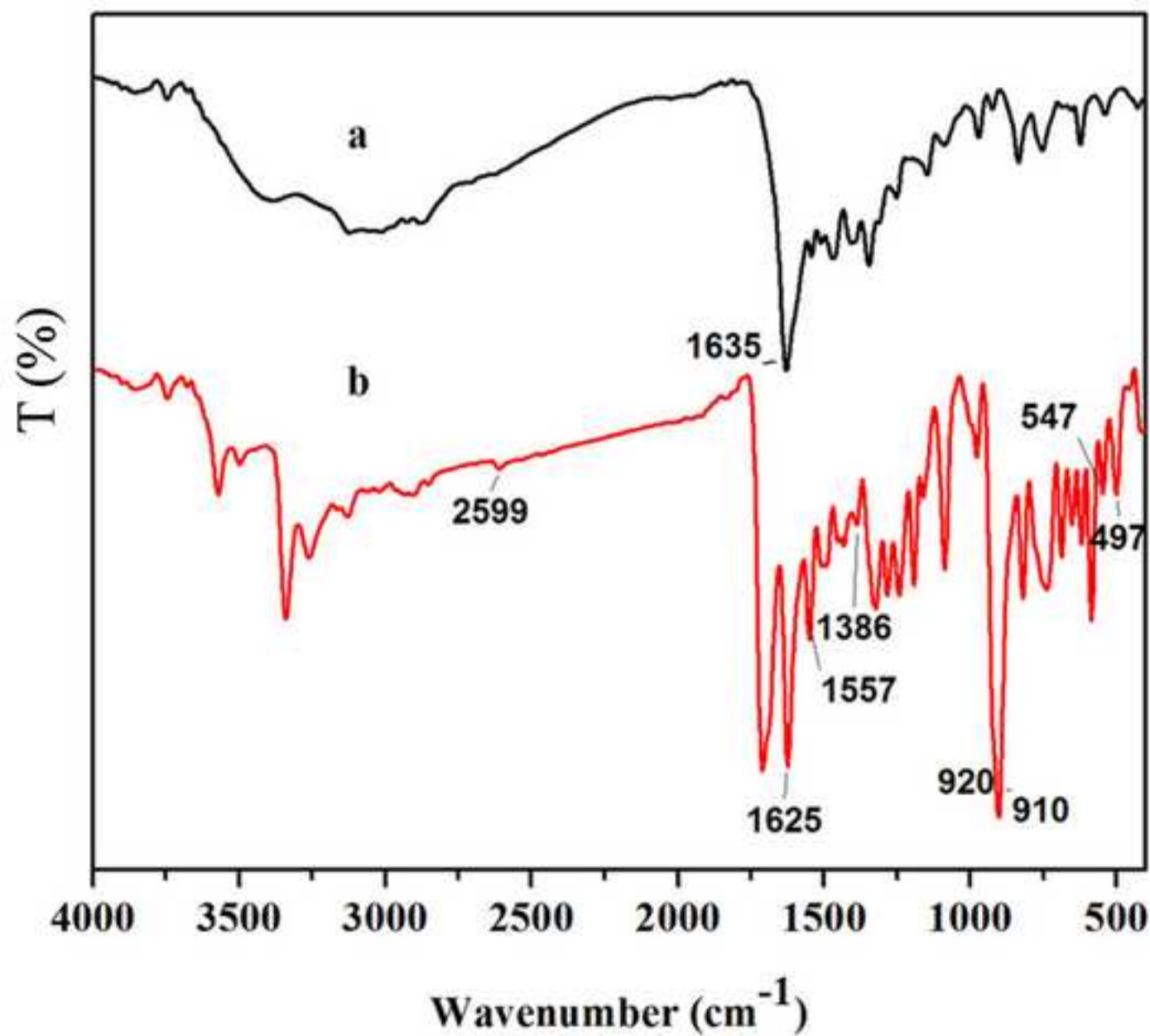
**Table 3**Hydrogen bond distances (Å) and angles (°) for [MoO<sub>2</sub>(Naph-His)].

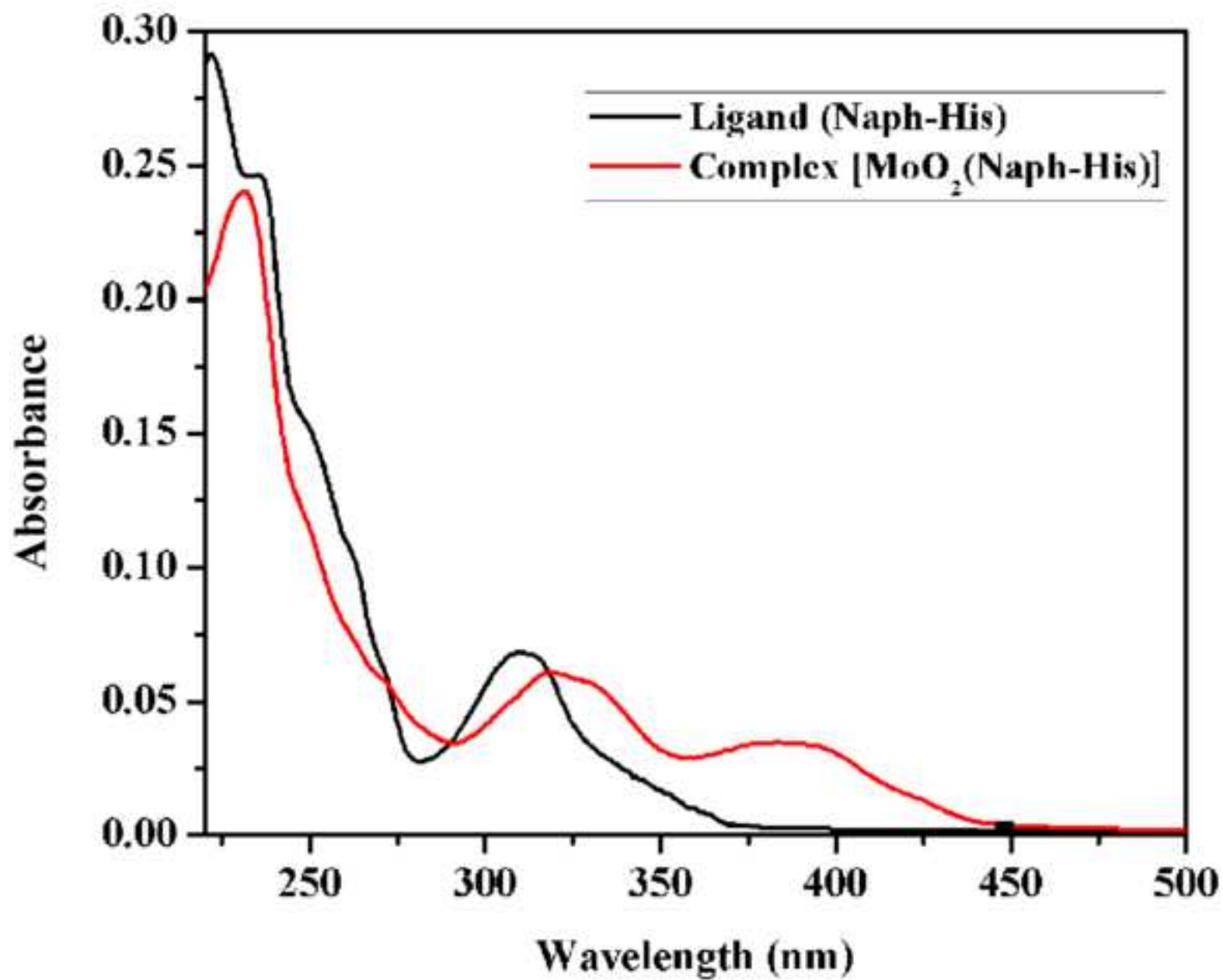
Donor --- H...Acceptor	D - H	H...A	D...A	D - H...A
C(2)...H(2)...O(4)	0.98	2.58	3.190(6)	121
C(14)...H(14B)...O(4)	0.97	2.59	3.382(6)	139
N(3)...H(3A)...O(2)	0.86	2.11	2.9441	164
N(3)--H(3A)...O(1)	0.86	2.58	2.9743	109

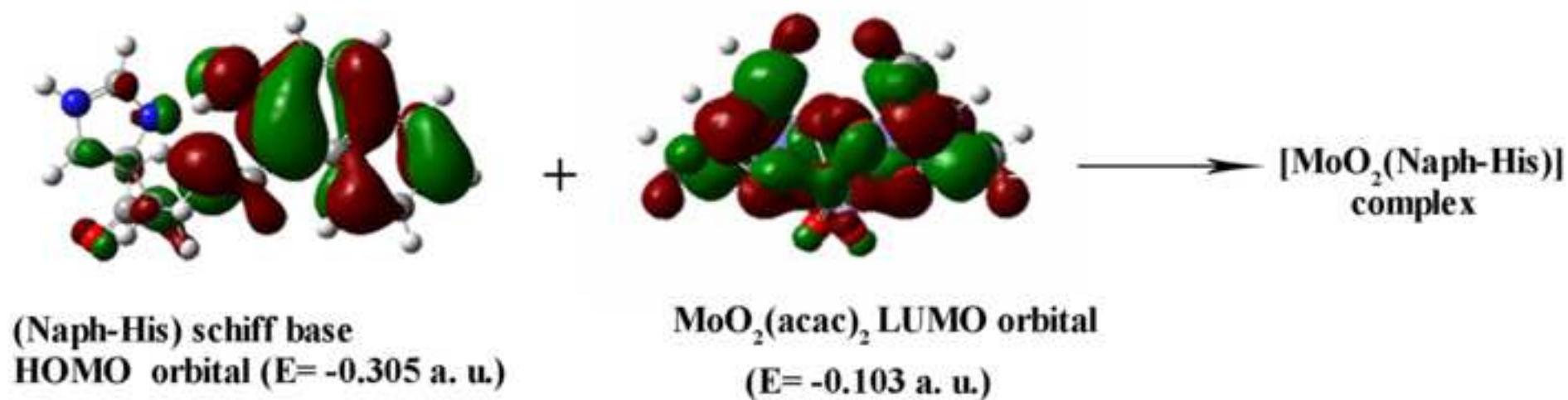


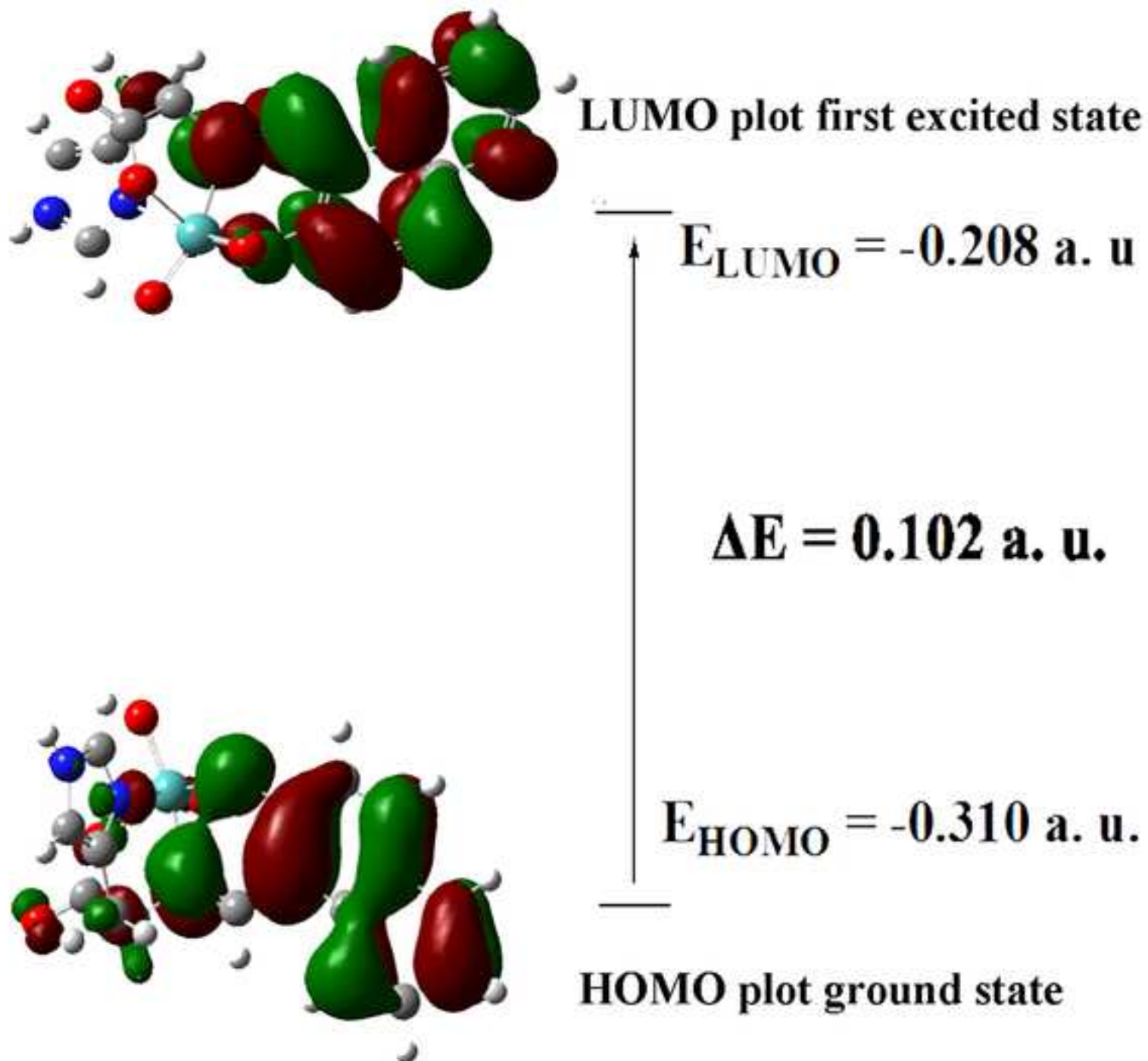


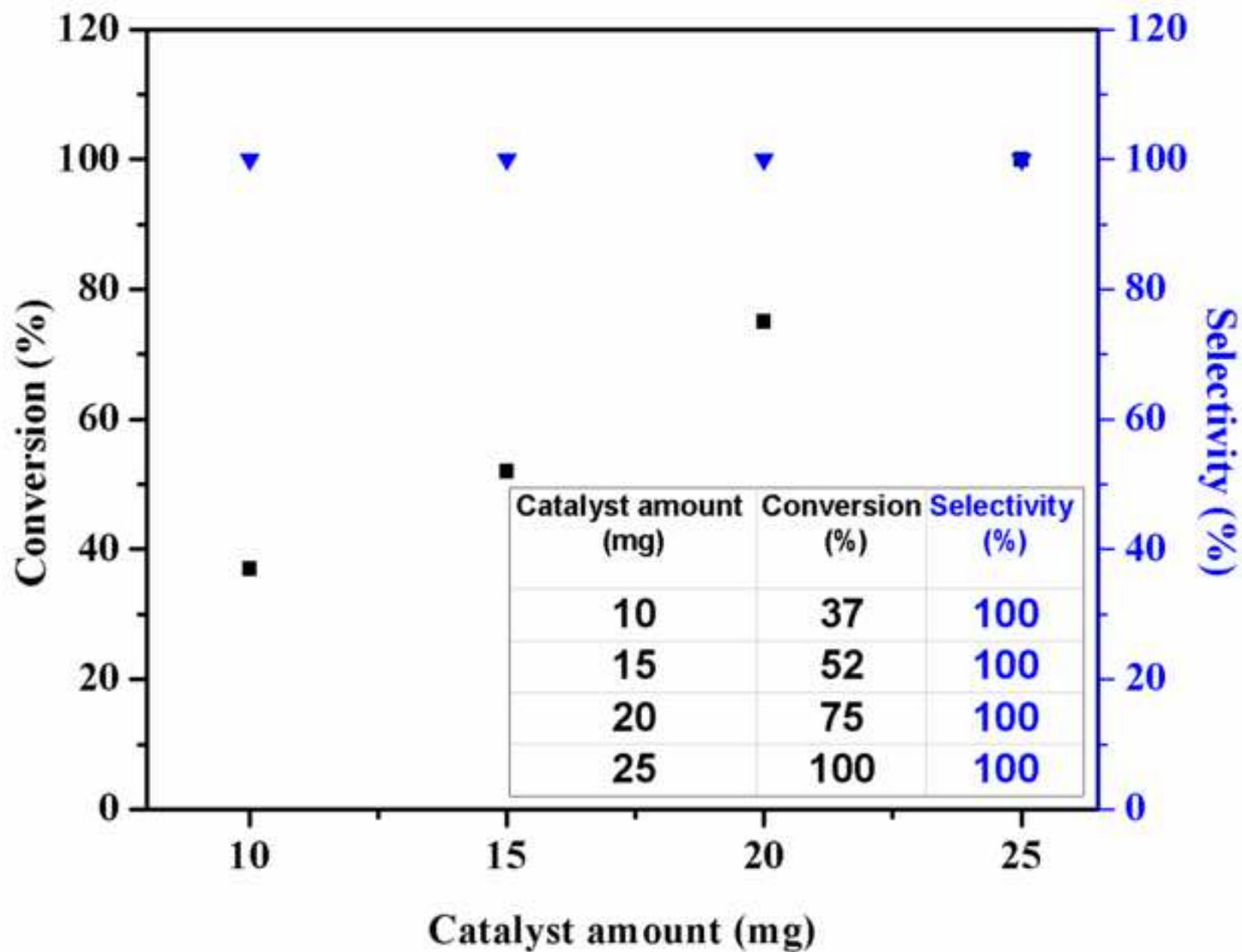


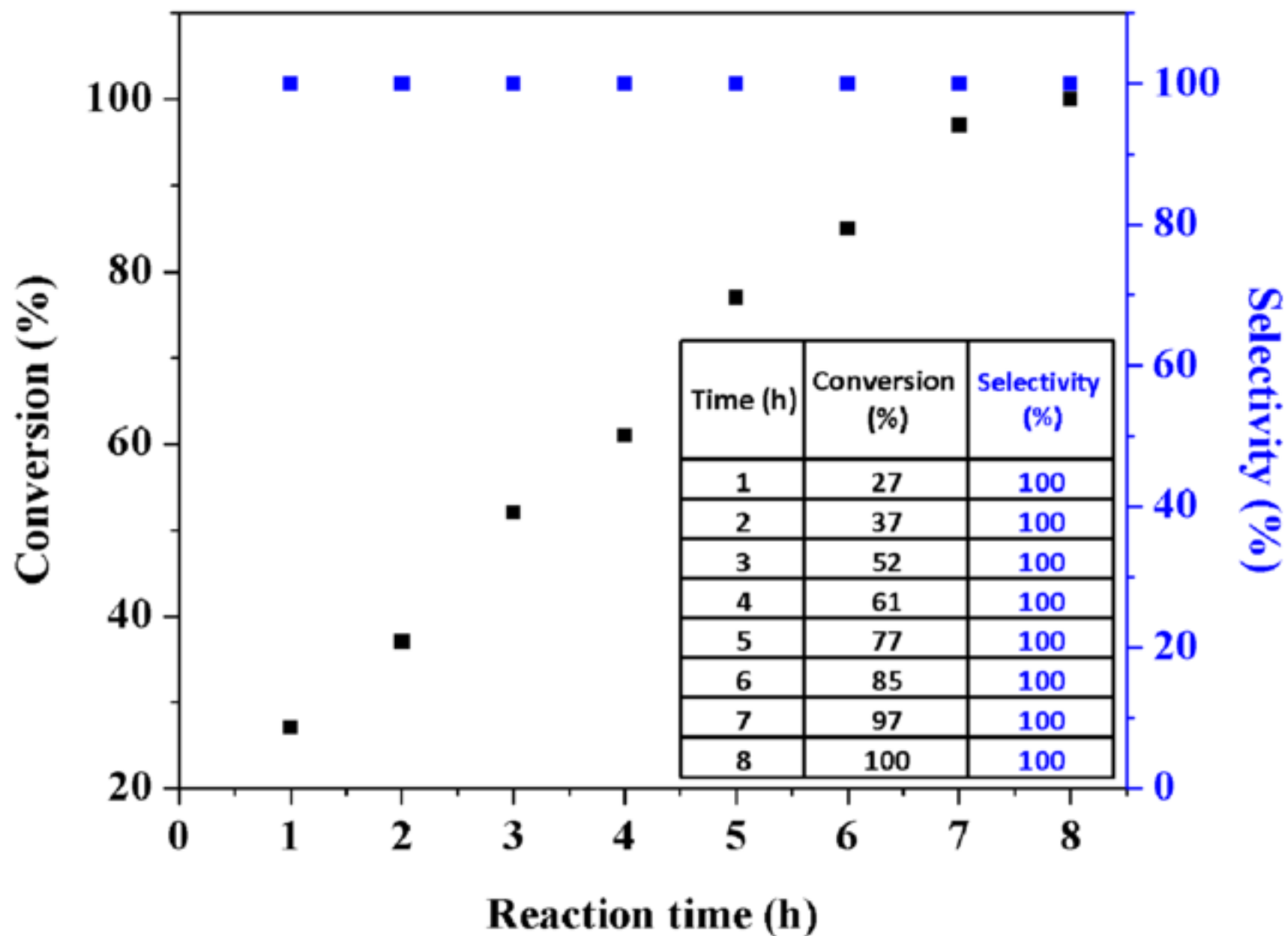


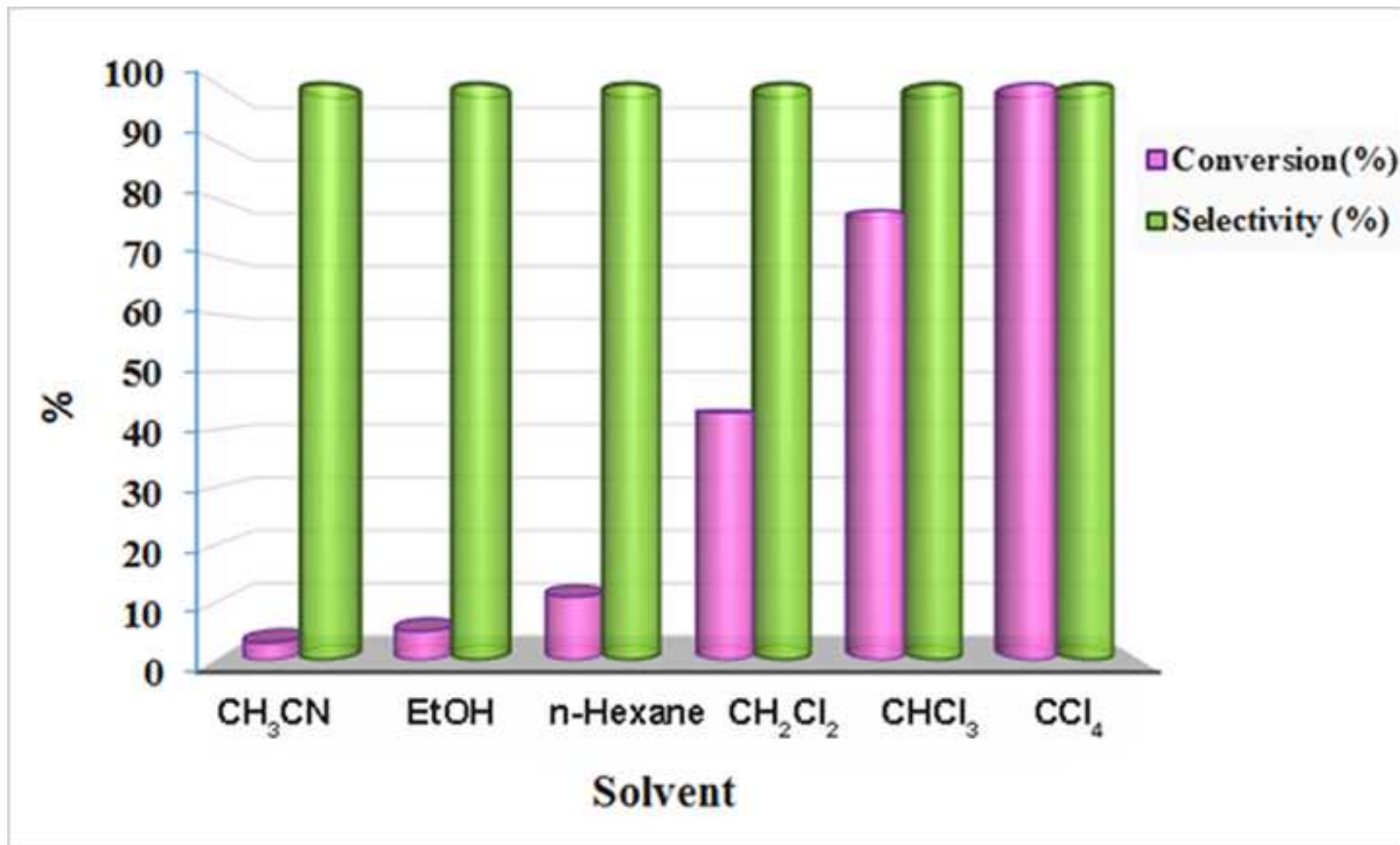




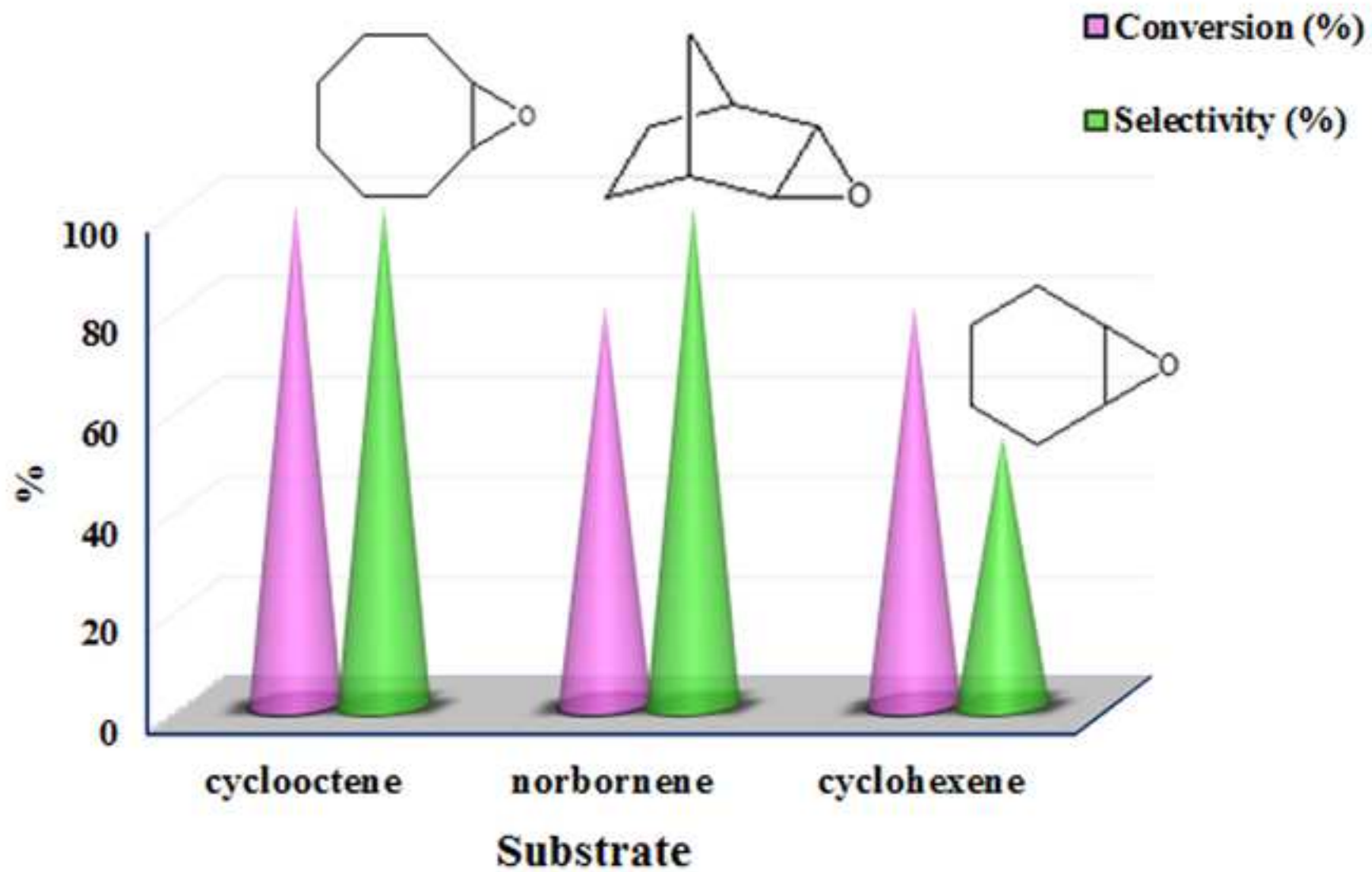




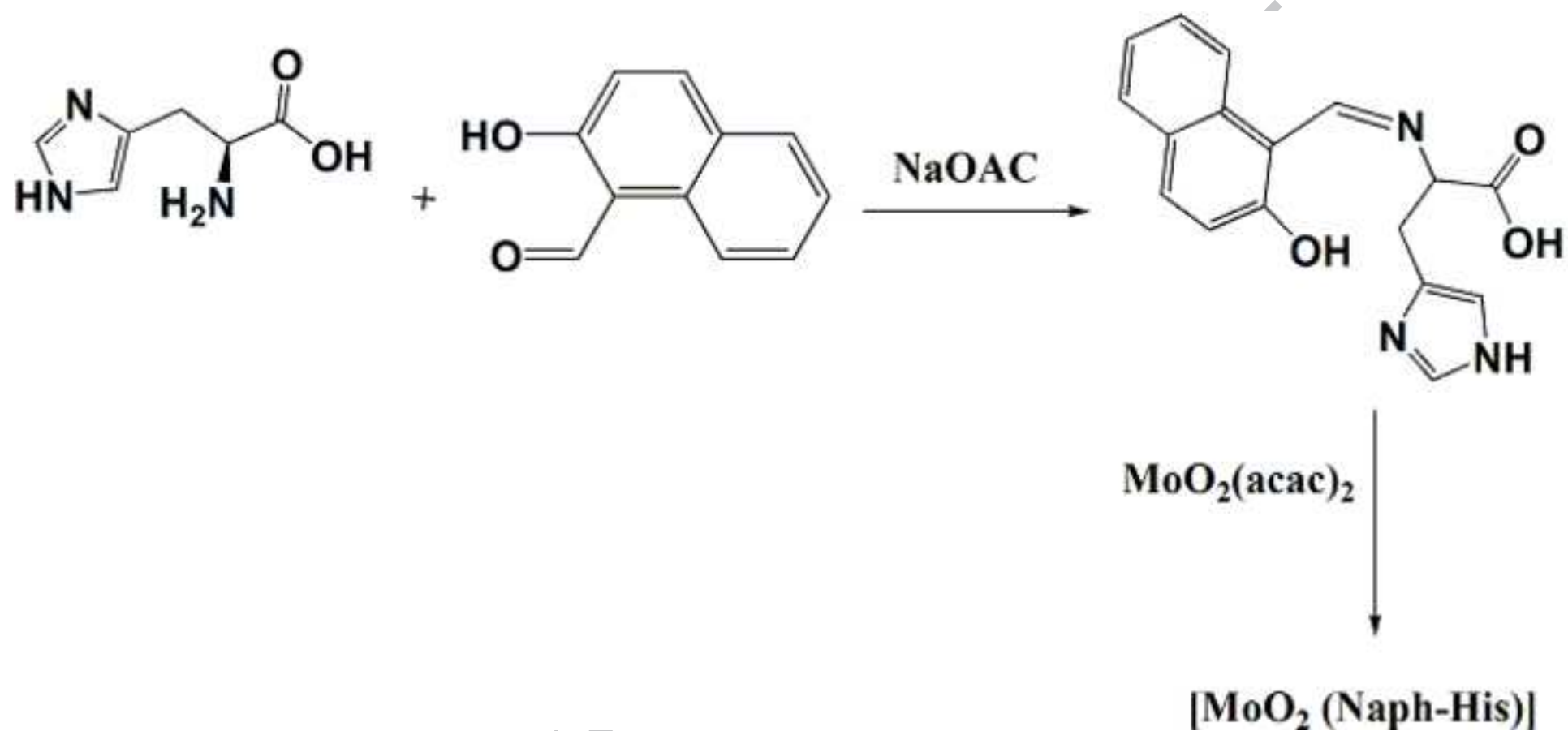


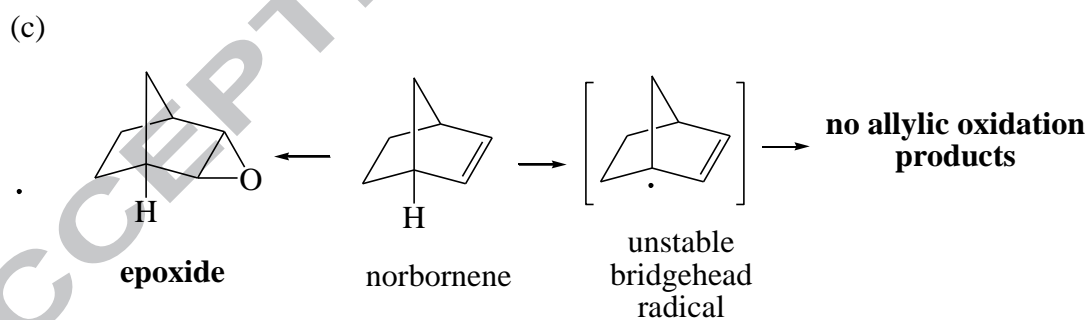
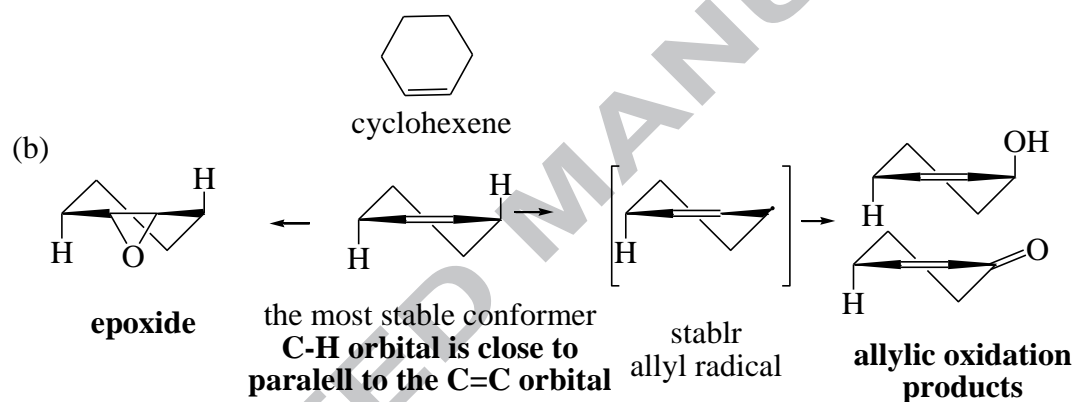
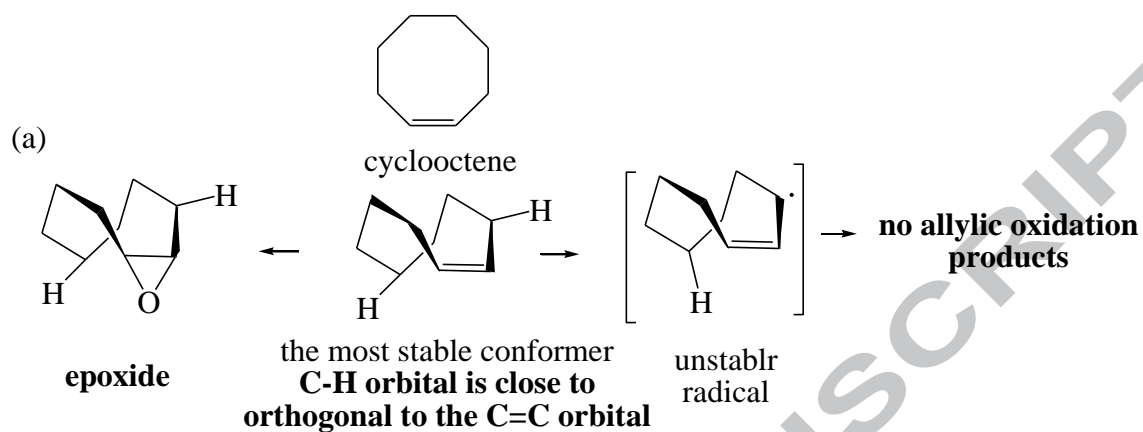








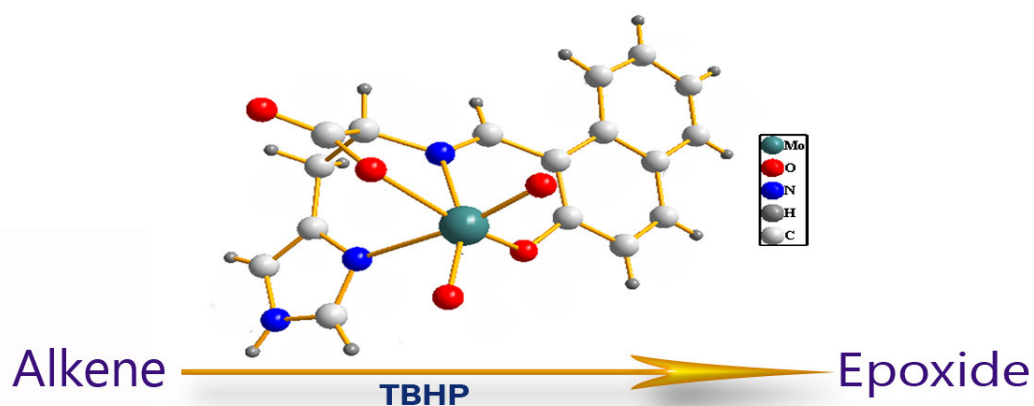




Graphical abstract pictogram:

**Synthesis, crystal structure and DFT studies of a new dioxomolybdenum(VI) Schiff base complex as an olefin epoxidation catalyst**

Zeinab Asgharpour, Faezeh Farzaneh\*, Alireza Abbasi, Mina Ghiasi



**Graphical abstract synopsis:**

The synthesis, characterization, crystal structural and DFT studies of a new Mo complex using  $\text{Mo}(\text{acac})_2$  and a Schiff base ligand derived from 2-hydroxy-1-naphthaldehyde and L-histidine in ethanol and its usage as an epoxidation catalyst are presented.